Article

Discovery of *ETS1* as a New Gene Predisposing to Dilated Cardiomyopathy

Zun-Ping Ke [*] , Jia-Ning Gu , Chen-Xi Yang , Xue-Lin Li , Su Zou , Yi-Zhe Bian , Ying-Jia Xu , Yi-Qing Yang [*]

Article

Discovery of *ETS1* as a New Gene Predisposing to Dilated Cardiomyopathy

Zun-Ping Ke [1],*, Jia-Ning Gu [2], Chen-Xi Yang [2], Xue-Lin Li [1], Su Zou [2], Yi-Zhe Bian [2], Ying-Jia Xu [2] and Yi-Qing Yang [2,3,4,*]

[1] Department of Geriatrics, Shanghai Fifth People's Hospital, Fudan University, Shanghai 200240, China

[2] Department of Cardiology, Shanghai Fifth People's Hospital, Fudan University, Shanghai 200240, China

[3] Department of Central Laboratory, Shanghai Fifth People's Hospital, Fudan University, Shanghai 200240, China

[4] Department of Cardiovascular Research Laboratory, Shanghai Fifth People's Hospital, Fudan University, Shanghai 200240, China

* Correspondence: kzprenmin@163.com (Z.-P.K.); yangyiqing@fudan.edu.cn (Y.-Q.Y.);
Tel.: +86-21-24289470 (Z.-P.K.); +86-21-24289657 (Y.-Q.Y.)

Abstract

Background/Objectives: Dilated cardiomyopathy (DCM), defined as dilation and contractile dysfunction of the left or both cardiac ventricles, remains the most common category of primary myocardial disease worldwide. It is the most prevalent cause of chronic heart failure and the most common indication for cardiac transplantation in young subjects. Accumulating evidence increasingly highlights the substantial genetic defects underlying DCM. Nevertheless, the genetic ingredients accountable for DCM in a larger percentage of cases remain indefinite. **Methods:** In the present research, a multigenerational pedigree suffering from DCM and a cohort of 276 healthy volunteers employed as control individuals were recruited from the Chinese Han-ethnicity population. A whole-exome sequencing (WES) assay followed by a Sanger sequencing analysis of the genomic DNAs from the available family members was implemented. Functional characterization of the identified genetic variant was conducted by utilizing a dual-luciferase analysis system. **Results:** A novel heterozygous variation in the *ETS1* (erythroblast transformation-specific 1) gene, NM_005238.4:c.447T>G;p.(Tyr149*), was identified by WES and validated by Sanger sequencing analysis to co-segregate with DCM in the whole DCM family. This nonsense *ETS1* variant was not found in 276 control subjects. Functional decipher elucidated that Tyr149*-mutant ETS1 failed to transactivate its representative target genes *CLDN5* (claudin 5) and *ALK1* (activin receptor-like kinase 1), two genes crucial for cardiovascular embryonic development and postnatal structural remodeling. **Conclusions:** The current investigation reveals *ETS1* as a novel gene predisposed to human DCM and indicates *ETS1* haploinsufficiency as an alternative molecular pathogenesis underlying DCM, providing a potential molecular target for the genetic counseling and early diagnosis as well as personalized prophylaxis of DCM.

Keywords: cardiomyopathy; medical genetics; functional genomics; transcription factor; ETS1; reporter gene assay

1. Introduction

Dilated cardiomyopathy (DCM), which is clinically characterized by progressive enlargement and systolic dysfunction of the left or both cardiac ventricles without a known secondary cause such as valvular heart disease, coronary artery disease, metabolic derangement, essential hypertension, infiltrative disease, viral infection, nutrient deficiency, exposure of medications and toxins, autoimmune disease, and any more, represents the most prevalent category of primary myocardial disorder in humans worldwide, occurring in up to 0.45% of the general population [1–3]. There exists

a slight woman preponderance in the prevalence of DCM, with an estimated male-to-female ratio of 3:4 [2]. DCM is associated with substantially enhanced risks for many detrimental clinical sequelae, encompassing ischemic stroke/thromboembolic complications [4–6], cardiac conduction block/abnormality [7–9], atrial fibrillation [10–12], chronic congestive heart failure [13–18], fatal/malignant ventricular dysrhythmias [19–21], and even cardiac demise [22–24]. In fact, in young individuals, DCM is the most prevalent cause of congestive heart failure and the most frequent indication for cardiac transplantation globally [25]. According to an observational study, approximately 26% of children with DCM experience either cardiac death or the necessity for a cardiac organ transplant within one year after initial diagnosis of DCM, with an additional increase of 1% per year thereafter [26]. Additionally, in adults aged 20–60 years, DCM is also the most common etiology of congestive/chronic heart failure and cardiac death, and the leading reason for heart transplant worldwide [25]. According to recent long-term studies of patients affected with non-ischemic DCM, about 50% suffered from a composite of unplanned cardiovascular hospitalization, life-threatening/non-fatal arrhythmia, or cardiovascular demise over 12 years [27], and roughly 17% underwent cardiac death, heart transplant, or implantation of ventricular assist device over 8 years [28]. Only in the United States, each year DCM causes approximately 46,000 hospitalizations and 10,000 deaths [29]. Consequently, DCM leads to substantial morbidity and mortality, and confers a tremendous socioeconomic burden on humans, underscoring the pressing need to unravel the causes underpinning DCM.

The etiology of DCM is extremely complex and highly diverse, and both exogenous/nonheritable risk factors and endogenous/genetic defectives may give rise to DCM [1,2,30,31]. Well-known acquired risk factors contributing to DCM include toxic chemicals (such as alcohol, clozapine, anabolic/adrenergic steroids, amphetamines, and anthracyclines), hemodynamic/mechanical factors (such as regurgitant/stenotic heart valve disease, anemia, athleticism/exercise, atrial tachycardias, premature ventricular beats, myocardial infarction/coronary artery disease, and pregnancy), inflammatory/infiltrative factors (such as immune myocarditis, pathogen myocarditis, and cardiac amyloidosis), endocrine/metabolic factors (such as diabetes mellitus, Cushing disease, acromegaly, pheochromocytoma, hypothyroidism, hyperlipidemia, and hyperthyroidism), hypertension, obesity, nutritional deficiency, obstructive sleep apnea, chronic kidney disease, hepatic cirrhosis, neuromuscular disease, severe sepsis, thoracic radiotherapy, and smoking [30,31]. However, there come fast-growing data convincingly suggesting the pivotal role of heritable determinants in the development of DCM, especially for familial DCM, which is defined as the presence of ≥2 relatives with DCM or the presence of one relative with DCM along with sudden cardiac death before the age of 35 years [1,2]. It is reported that around 30% of DCM is familial [31], and in up to 50% of DCM patients, DCM is transmitted in an autosomal-dominant mode, though less common patterns of transmissions, encompassing X-linked recessive inheritance and autosomal-recessive inheritance as well as mitochondrial inheritance, have also been reported in some DCM cases [32]. To date, DCM-causing variations in >250 genes implicated in many distinct cellular processes have been identified, which include genes involved in force generation (sarcomere, Z-disk, sarcolemma, and intercalated disc proteins), cellular architecture (cytoskeleton, nuclear envelope, and desmosome proteins), gene expression (transcription factors and RNA-binding proteins), energy regulation (mitochondria), electrolyte homeostasis (ion channels and gap junction channels), and signaling transduction [1,2,33–61]. Notably, genetic defects responsible for DCM are discovered much more commonly in pediatric cases (54%) than in adult patients (27%) [2] Nevertheless, these known genetic determinants account for 25%–50% of all DCM cases, strongly indicating that additional genetic components responsible for DCM remain to be identified [1,2,25].

2. Materials and Methods

2.1. Ethical Approval

The present human research project was implemented in strict compliance with the tenets outlined in the Helsinki Declaration issued by the World Medical Association. The institutional medical ethics committee of Shanghai Fifth People's Hospital affiliated to Fudan University approved the research protocols (ethical approval No. 2020-011) that were applied to the current human research. Prior to commencing recruitment for the current research, all candidate research participants or their legal guardians signed informed consent forms to fulfil clinical and genetic analyses.

2.2. Recruitment and Clinical Characterization of Research Participants

For the present investigation, a 42-member pedigree across five generations affected with DCM was identified from the Chinese Han-race population (arbitrarily termed as Family DCM-101), from which available pedigree members were recruited. As control subjects, a cohort of 276 unrelated healthy volunteers with no family history of heart disease was enlisted from the same population in the same geographical area. All research participants underwent a comprehensive clinical assessment, including a thorough review of anamnestic personal and familial histories as well as medical history, an elaborate physical examination, a transthoracic echocardiographic imaging, and a standard 12-lead electrocardiography, along with routine laboratory tests. All DCM patients underwent a maximal exercise performance test. However, standard cardiac magnetic resonance imaging, coronary computed tomography angiography, and an endomyocardial biopsy were performed only when strongly indicated. As previously described [37], DCM was diagnosed by the existence of a left-ventricular end-diastolic diameter >117% of the predicted value adjusted for age and body surface area, and fractional shortening <25% or ejection fraction <45%, in the conditions of no significant obstructive coronary artery disease, sustained arterial hypertension, valvular heart disease, documented myocarditis, and systemic disorders. A total of 3 mL of peripheral venous blood samples was collected from each study individual and stored in a collecting tube containing an anticoagulant (acid-citrate dextrose) in a low-temperature (–80℃) refrigerator. Extraction of genomic DNA from research participants' whole blood leucocytes was conducted utilizing the QIAamp® DNA Blood Mini Kit (Cat. No. 51106; QIAGEN GmbH, Hilden, Germany).

2.3. Genetic Analysis of Research Participants

As described previously [62–66], a whole-exome sequencing (WES) assay was performed on genomic DNA samples from selected affected and unaffected members of Family DCM-101 suffering from DCM. Briefly, a sample of 5 µg of genomic DNAs from a family member chosen for WES was randomly sheared via the Covaris® S2 Ultrasonicator (Covaris, Woburn, MA, USA) to generate various sizes of DNA fragments with a major length distribution of 100 to 500 bp, which were ligated with sequencing adapters and captured using the SureSelect[XT] Human All Exon V6 Kit (Cat. No. 5190-8864; Agilent Technologies, Santa Clara, CA, USA) to obtain a whole-exome library. The exomic DNA library was sequenced on the Illumina HiSeq® 4000 platform (Illumina, San Diego, CA, USA). Bioinformatic analyses of the sequence datasets produced by WES was implemented as narrated elsewhere [62–66]. In brief, alignment of read data to the referential human genome (build GRCh37/hg19) was implemented after removing low-quality reads by employing the Burrows–Wheeler Aligner (BWA; version 0.7.17) software package [67]. Thereafter, duplicated reads were ruled out, and the Genome Analysis Toolkit (GATK; version 3.8.1.0) software [68] was applied to call sequence variations (small insertions and deletions as well as single-nucleotide polymorphisms) at the targeted regions of an individual genome. All genetic variants were annotated by the ANNOVAR (version 2015) program [69]. Non-synonymous variations, along with splicing donor/acceptor variations, were subject to further examination, encompassing a Sanger sequencing assay of a gene with a deleterious variation and a segregation assay among all the family members from Family

DCM-101. Once a gene harboring a DCM-causing mutation was discovered by WES assay in Family DCM-10-1, a Sanger sequencing assay of the same gene (including the entire coding exons as well as all splicing junction sites) was performed in 276 unrelated control persons. Additionally, for each identified genetic variation, the Single Nucleotide Polymorphism database (dbSNP; https://www.ncbi.nlm.nih.gov/, accessed on 20 June 2025) and the Genome Aggregation Database (gnomAD; http://gnomad-sg.org/, accessed on 20 June 2025) were consulted to verify its novelty.

2.4. Recombination of Gene Expression Plasmids

A**s** depicted elsewhere [70–72], total mRNAs were purified from human myocardial tissue specimens, from which cDNAs were yielded by routine reverse transcription of total mRNAs. A 1700-bp cDNA fragment containing the full-length ORF as well as partial 5′- and 3′ untranslation regions of the wild-type human erythroblast transformation-specific 1 (*ETS1*) gene (https://www.ncbi.nlm.nih.gov/nuccore/NM_005238.4) was amplified from the purified human heart cDNA by polymerase chain reaction (PCR) using the Platinum™ SuperFi II DNA Polymerase (Cat. No. 12361050; Invitrogen, Carlsbad, CA, USA) and a specific pair of oligonucleotide primers of 5′-GTCGCTAGCGAGATCGAGAGCGAACGAGG-3′ (forward) and 5′-GTCGCGGCCGCACCAACACGGCTGTCCTTGG-3′ (reverse). The produced *ETS1* cDNA was purified with the QIAEX II Gel Extraction Kit (Cat. No. 20051; QIAGEN GmbH, Hilden, Germany). The purified *ETS1* cDNA and eukaryotic expression plasmid pCI-neo (Cat. No. E1841; Promega, Madison, WI, USA) were doubly cut with restriction endonucleases *Nhe*I (Cat. No. ER0971; Thermo Scientific, Waltham, MA, USA) and *Not*I (Cat. No. ER0595; Thermo Scientific, Waltham, MA, USA), purified employing the GeneJET™ Gel Extraction Kit (Cat. No. K0692; Thermo Scientific, Waltham, MA, USA), and ligated by T₄ DNA ligase (Cat. No. 15224041; Invitrogen, Waltham, MA, USA) to create the wild-type human ETS1-pCI plasmid ETS1-pCI. With the wild-type human ETS1-pCI plasmid used as a template, the Tyr149*-mutant ETS1-pCI expression plasmid was generated through site-targeted mutagenesis utilizing the GENEART® Site-Directed Mutagenesis System (Cat. No. K0692; A13282; Invitrogen, Waltham, MA, USA) with the complementary primer pairs of 5′-AGTCAACCCAGCCTAGCCAGAATCCCGCTAT-3′ (forward) and 5′-ATAGCGGGATTCTGGCTAGGCTGGGTTGACT-3′ (backward) and was validated by direct Sanger sequencing assay. In addition, a 1101-bp promoter fragment (from −919 upstream of the transcriptional initial site to +182, with the first transcribed nucleotide numbered as +1) of the human claudin 5 (*CLDN5*) gene (https://www.ncbi.nlm.nih.gov/nuccore/NC_000011.10?from=128458765&to=128587558&report=genbank&strand=true) was amplified from a template of human genomic DNA by PCR with the DreamTaq™ DNA Polymerase (Cat. No. EP1702; Thermo Scientific, Waltham, MA, USA) and a *CLDN5*-specific pair of primers of 5′-CTAGGTACCGGAGGCCGCAGCAGTCATCC-3′ (forward) and 5′-CTAAAGCTTCTCAATCTTCACAGGGGCTG-3′ (backward). The amplified *CLDN5* promoter DNA and the reporter vector pGL3-Basic (Cat. No. E1751; Promega, Madison, WI, USA) were doubly digested by restriction enzymes *Kpn*I (Cat. No. ER0521; Thermo Scientific, Waltham, MA, USA) and *Hind*III (Cat. No. ER0501; Thermo Scientific, Waltham, MA, USA), separated by agarose gel electrophoresis, extracted with the GenElute™ Gel Extraction Kit (Cat. No. NA1111; Sigma-Aldrich, St. Louis, MO, USA), and ligated with T4 DNA ligase (Cat. No. 15224041; Invitrogen, Waltham, MA, USA) to construct the CLDN5-luciferase (CLDN5-luc) reporter vector, which expresses firefly luciferase. Similarly, a 1690-bp promoter fragment (from −221 to −1910 upstream of the transcriptional initial site) of the human activin receptor-like kinase 1 (*ALK1*) gene https://www.ncbi.nlm.nih.gov/nuccore/NC_000012.12?from=51906944&to=51923361&report=genbank) was amplified from a template of human genomic DNA by PCR with the DreamTaq™ DNA Polymerase (Cat. No. EP1702; Thermo Scientific, Waltham, MA, USA) and an *ALK1*-specific pair of primers of 5′-GATGGTACCGACTCTCGCTTCTCAGGAC-3′ (forward) and 5′-GATAAGCTTCGCACCCGGGCCGGGCCTCC-3′ (backward). The amplified *ALK1* promoter DNA and the reporter vector pGL3-Basic (Cat. No. E1751; Promega, Madison, WI, USA) were doubly cut

by restriction enzymes *Kpn*I (Cat. No. ER0521; Thermo Scientific, Waltham, MA, USA) and *Hind*III (Cat. No. ER0501; Thermo Scientific, Waltham, MA, USA), separated by agarose gel electrophoresis, extracted with the GenElute™ Gel Extraction Kit (Cat. No. NA1111; Sigma-Aldrich, St. Louis, MO, USA), and ligated with T4 DNA ligase (Cat. No. 15224041; Invitrogen, Waltham, MA, USA) to construct the ALK1-luciferase (ALK1-luc) reporter vector, which expresses firefly luciferase. All the final recombinant expression plasmids were subject to confirmation by Sanger sequencing analysis.

2.5. Cell Transfection and Dual-Reporter Gene Analysis

As narrated previously [37,73,74], HeLa cells (Cat. No. SCSP-504; National Collection of Authenticated Cell Cultures, Shanghai, China) were seeded into a Nunc™ 24-well microplate/multidish (Cat. No. 144530; Thermo Fisher Scientific, Rochester, NY, USA) at a density of 1×10^5 cells/well, and routinely cultivated for 24 h before transiet transfection with appropriate amounts of various expression plasmids using the Lipofectamine™ 3000 Transfection Reagent (Cat. No. L3000015; Invitrogen; Waltham, MA, USA). Specifically, HeLa cells were transiently transfected with 200 ng of empty pCI, or 200 ng of wild-type ETS1-pCI, or 200 ng of Tyr149*-mutant ETS1-pCI, or 100 ng of empty pCI plus 100 ng of wild-type ETS1-pCI, or 100 ng of wild-type ETS1-pCI plus 100 ng of Tyr149*-mutant ETS1-pCI, in combination with 10 ng of pGL4.75 (Cat. No. E6931; Promega, Madison, WI, USA) and 1000 ng of CLDN5-luc or ALK1-luc. The pGL4.75 vector (Cat. No. E6931; Promega, Madison, WI, USA) expressing renilla luciferase was co-transfected as an internal control to balance transfection efficiency. HeLa cells were collected 36 h post-transfection, lysed, and the promoter-driven luciferase activities were quantitatively detected under the GloMax® Discover System (Promega, Madison, WI, USA) by utilizing the Dual-Glo® Luciferase Assay System (Cat. No. E2920; Promega, Madison, WI, USA), as per the manufacturer's instructions. The promoter activity was measured as the ratio of firefly:renilla luciferase luminescence intensity. Each recombinant expression plasmid, along with an internal control plasmid, was transiently transfected and detected three times in triplicate. Results are expressed as means of relative luciferase activities from three independent transfection experiments and standard deviations (SD).

2.6. Statistical Analysis

Continuous data of promoter activities are presented as mean ± SD. All data were analyzed by using the Student's unpaired *t*-test for pairwise comparison or analysis of variance (ANOVA) followed by Tukey-Kramer HSD post-hoc test for multi-group analysis. Differences were considered to be statistically significant at two-tailed *p*-values of <0.05.

3. Results

3.1. Demographic and Phenotypic Characteristics of the Studied Family Affected with DCM

For the current investigation, as illustrated in Figure 1, a 42-member pedigree affected with DCM spanning five generations was identified as Family DCM-101 from the Chinese Han-ethnicity population. In this 42-member family with DCM, there were 37 living members available, including 19 male members and 18 female members. The proband of Family DCM-101 (IV-3) was first diagnosed with DCM at the age of 41 years. During the proband's clinical follow-up, he experienced progressive fatigue and dyspnea on exertion, left ventricular dilation and systolic dysfunction on echocardiograms ,   and received pharmacologic therapies (intravenous injections, infusions and oral medications) for chronic cardiac failure, encompassing diuretics (furosemide and spironolactone), angiotensin-converting enzyme inhibitor (captopril), and β-adrenergic receptor antagonist (metoprolol). His grandfather (II-1) and two other relatives (II-3 and I-1) had a past medical history of DCM and died of progressive congestive heart failure attributable to DCM. His grandmother (II-2) and another relative (I-2) had no medical history of DCM and died of a cerebral stroke.
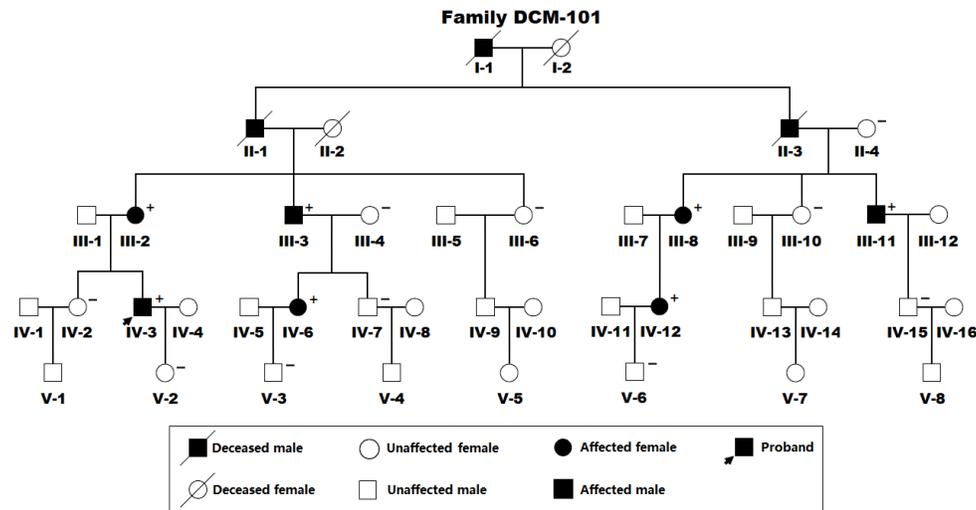
Figure 1. The pedigree of the studied family suffering from dilated cardiomyopathy. Family members are identified by generation and number (using a Roman and an Arabic numeral, respectively). "+" denotes a carrier of the detected *ETS1* mutation in a heterogeneous status; "−" means a non-carrier.

Additionally, in Family DCM-101, all 10 affected members were diagnosed with DCM based on clinical symptoms, physical signs, and echocardiographic findings, while all unaffected members denied a medical history of DCM, with normal echocardiograms. No members from Family DCM-101 had known environmental pathogenic factors predisposing to DCM, encompassing viral myocarditis, coronary heart disease, autoimmune disorders, rheumatic heart disease, and arterial hypertension. A genetic evaluation of the family (Family DCM-101) revealed that DCM was inherited as an autosomal-dominant trait in the whole pedigree, with complete penetrance. Notably, all 10 affected members also suffered mild facial dysmorphisms, including a high forehead, a broad nasal bridge with bulbous tip, and dysplastic little ears. Besides, in addition to DCM, three family members (III-8, III-11, and IV-12) also had atrial fibrillation, and one family member (IV-6) also had a minor membranous ventricular septal defect (VSD) that closed spontaneously within the first year of her life. The demographic and baseline phenotypic characteristics of the living family members with DCM from Family DCM-101 are outlined in Table 1.

Table 1. Demographic and baseline phenotypic characteristics of the affected pedigree members alive from Family DCM-101.

Individuals (Family DCM-101)	Sexes	Ages (years)	Cardiac Phenotypes	LVEDD (mm)	LVESD (mm)	LVEF (%)	LVFS (%)
III-2	Female	68	DCM	71	62	33	18
III-3	Male	65	DCM	76	65	30	14
III-8	Female	63	DCM, AF	70	60	27	13
III-11	Male	57	DCM, AF	69	58	32	16
IV-3	Male	45	DCM	58	48	36	18
IV-6	Female	40	DCM, VSD	64	52	38	19
IV-12	Female	38	DCM, AF	60	50	40	20

DCM, dilated cardiomyopathy; LVEF, left ventricular ejection fraction; AF, atrial fibrillation; LVESD, left ventricular end-systolic diameter; VSD, ventricular septal defect; LVEDD, left ventricular end-diastolic diameter; LVFS, left ventricular fractional shortening.

3.2. Discovery of a New DCM-Causative Mutation in ETS1

A WES assay was completed in four DCM-affected members (III-2, III-8, IV-3 and IV-12 from Family DCM-101) and three unaffected members (IV-2, V-2 and V-6 from Family 1), which yielded

about 22 Giga bases of DNA sequence data per family member, presenting a nearly 97% coverage of the referential human genome (GRCh37/hg19) with approximately 76% mapped to the target regions. An average of 15,209 nonsynonymous variations (varying from 14,917 to 17,536) per family member passed filtering on the likely inheritance modes (the recessive genetic transmission pattern was also included during screening for potential candidate gene variations), of which 11 heterozygous missense and nonsense genetic variations passed filtering by ANNOVAR with a minor allele frequency of <0.01% and were carried by all the four DCM members (III-2, III-8, IV-3 and IV-12 from Family DCM-101) who had experienced WES analysis, as given in Table 2.

Table 2. Candidate genetic variations for dilated cardiomyopathy unveiled by an exome-wide sequencing assay.

Chr	Position (hg19)	Ref	Alt	Gene	Variation
1	92,184,903	G	A	_TGFBR3_	NM_003243.5: c.1532G>A; p.(Trp511*)
2	141,777,525	C	G	_LRP1B_	NM_018557.3: c.1936C>G; p.(His646Asp)
3	71,096,210	C	G	_FOXP1_	NM_032682.6: c.547C>G; p.(Gln183Glu)
4	157,693,868	A	G	_PDGFC_	NM_016205.3: c.673A>G; p.(Lys225Glu)
6	38,029,545	G	C	_ZFAND3_	NM_021943.3: c.289G>C; p.(Glu97Gln)
7	133,689,816	C	T	_EXOC4_	NM_021807.4: c.2500C>T; p.(Gln834*)
11	128,355,998	T	G	_ETS1_	NM_005238.4: c.447T>G; p.(Tyr149*)
12	66,773,093	G	T	_GRIP1_	NM_021150.4: c.2432G>T; p.(Ser811Ile)
15	86,266,500	C	G	_AKAP13_	NM_006738.6: c.6706C>G; p.(Leu2236Val)
16	49,671,508	T	C	_ZNF423_	NM_015069.5: c.1555T>C; p.(Cys519Arg)
18	34,092,506	G	A	_FHOD3_	NM_025135.5: c.511G>A; p.(Ala171Thr)

Chr, chromosome; Ref, reference; Alt, alteration.

Further Sanger sequencing assay of these genetic variations in all the family members available from Family DCM-101 revealed that only the heterozygous nonsense mutation of chr11:128,355,998T>G (GRCh37.p13/hg19: NC_000011.9), equivalent to chr11:128,560,220T>G (GRCh38.p14/hg38: NC_000011.10), or NM_005238.4:c.447T>G;p.(Tyr149*) in the erythroblast transformation-specific 1 (_ETS1_) gene, was verified to co-segregate with the DCM phenotype in the whole family, with complete penetrance, being shared by all DCM-affected members and absent in all unaffected members of Family DCM-101. However, Sanger sequencing assay of the other 10 genetic variations demonstrated that none co-segregated with the DCM phenotype in the whole family, suggesting that none of these 10 genetic variations is likely to underlie DCM in this family. In addition, a Sanger sequencing assay of the _ETS1_ gene in a total of 276 unrelated control people revealed no pathogenic mutations. The detected _ETS1_ mutation was absent in such genetics databases as dbSNP (accessed on 20 June 2025) and gnomAD (accessed on 20 June 2025), indicating it as a novel _ETS1_ mutation. The primers designed to specifically amplify the _ETS1_ gene (including the whole coding exons and splicing boundaries) by PCR were provided in Table 3.

Table 3. Primers to specifically amplify the coding exons and splicing boundaries of the _ETS1_ gene.

Coding exons	Forward primers (5'→3')	Reverse primers (5'→3')	Amplicon sizes (bp)
1	AAAGTCGGATTTCCCCCGTC	AGGGTTCTCGCTCATTTGGG	515
2	CTGGTGCTCTGGTGAGGATG	CTGGTGCTCTGGTGAGGATG	486
3	TTGGCTGGCAGTAGTGACCT	GGCACATTCCCACATACGTC	571
4	TCTTTAGACAAGGCCACAGTCA	TGGCCATCGTAGTGCACAGT	568
5	CATAGGGCCCTGTAGATGGTG	GGACTTGGCTAAAACACCACG	514
6	CCCAAACGCTACTCCGACAG	AAAGGGAGTCTCTCGTCGTC	664
7	GAAGAGGGATGTGGGAGTGC	CACAGGAGGCAGCTCTATGG	491
8	TTGTGACTCCCATCCTTGCC	GCTTTCCTTTCCCAACTGCG	609

The DNA sequence chromatograms illustrating the heterozygous mutant *ETS1* alleles (T/G) as well as wild-type *ETS1* alleles (T/T) are provided in Figure 2A. The schematic diagrams delineating the structural domains of the ETS1 protein are given in Figure 2B.
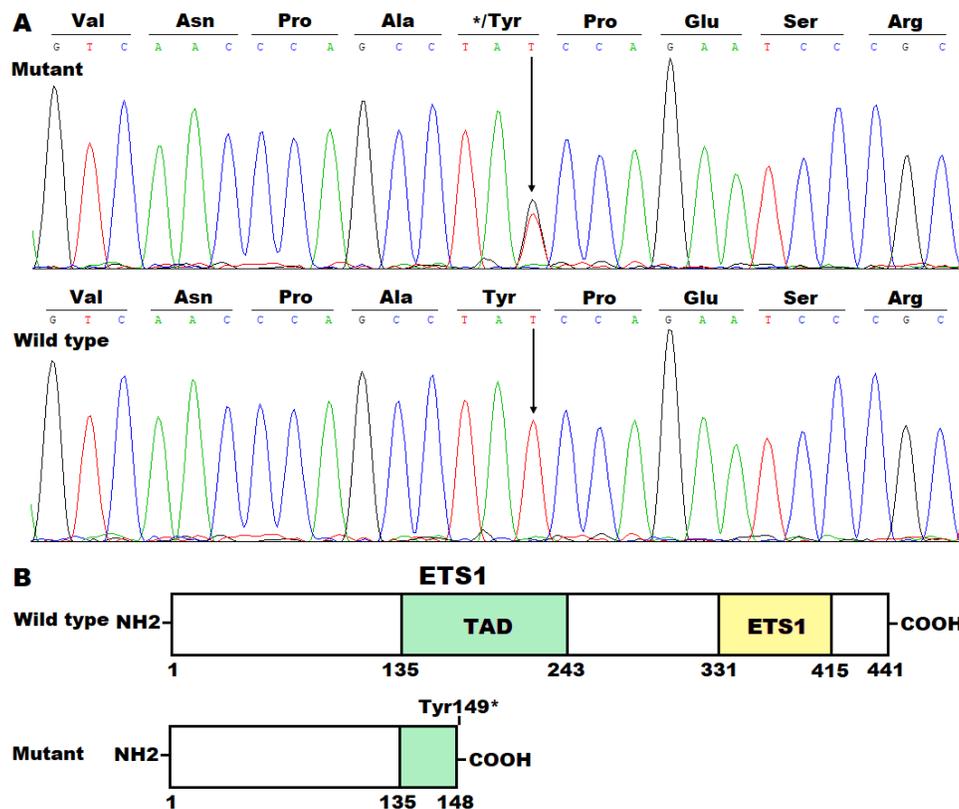

Figure 2. A novel *ETS1* mutation identified to account for familial dilated cardiomyopathy. (A) Sequence chromatograms demonstrated the heterogeneous mutant *ETS1* alleles (T/G) in the affected proband (mutant) and wild-type *ETS1* alleles (T/T) in an unaffected individual (wild type). An arrow points to where the mutation occurs in the proband's *ETS1* allele. (B) The schematic diagrams signified the structural domains of the ETS1 protein. ETS1, erythroblast transformation-specific 1; TAD, transcription activation domain.

3.3. Failure of Tyr149*-Mutant ETS1 to Transactivate CLDN5

As exhibited in Figure 3, in HeLa cells routinely cultivated in vitro and transiently transfected with various eukaryotic expression plasmids, the wild-type ETS1-pCI-neo plasmid and Tyr149*-mutant ETS1-pCI-neo plasmid induced transcriptional activation of the *CLDN5* promoter by ~28-fold and ~2-fold, respectively (Tyr149*-mutant ETS1-pCI-neo vs wild-type ETS1-pCI-neo: t = 15.8273; p = 0.0001). When the wild-type ETS1-pCI-neo and Tyr149*-mutant ETS1-pCI-neo plasmids were co-transfected, the elicited transactivation activity was ~15-fold (wild-type ETS1-pCI-neo vs wild-type ETS1-pCI-neo + Tyr149*-mutant ETS1-pCI-neo: t = 6.9335; p = 0.0023). When multiple-group comparisons were implemented, similar statistical data were obtained (F = 127.82, p = 1.534×10^{-8}). Multiple-group comparisons were performed between 200 ng of empty pCI-neo plasmid and 200 ng of wild-type ETS1-pCI-neo plasmid (t = 25.59, p <0.0001), between 200 ng of empty pCI-neo plasmid and 200 ng of Tyr149*-mutant ETS1-pCI-neo plasmid (t = 0.3533, p = 0.9989), between 200 ng of empty pCI-neo plasmid and 100 ng of empty pCI-neo plasmid + 100 ng of wild-type ETS1-pCI-neo plasmid (t = 15.4233, p <0.0001), between 200 ng of empty pCI-neo plasmid and 100 ng of wild-type ETS1-pCI-neo plasmid + 100 ng of Tyr149*-mutant ETS1-pCI-neo plasmid (t = 13.04, p <0.0001), between 200 ng of wild-type ETS1-pCI-neo plasmid and 200 ng of Tyr149*-mutant ETS1-pCI-neo plasmid (t = 25.9433, p <0.0001), between 200 ng of wild-type ETS1-pCI-neo plasmid and 100 ng of empty pCI-neo plasmid + 100 ng of wild-type ETS1-pCI-neo plasmid (t = 10.1667, p = 0.0002), between 200 ng of wild-type

ETS1-pCI-neo plasmid and 100 ng of wild-type ETS1-pCI-neo plasmid + 100 ng of Tyr149*-mutant ETS1-pCI-neo plasmid (t = 12.55, p <0.0001), between 200 ng of Tyr149*-mutant ETS1-pCI-neo plasmid and 100 ng of empty pCI-neo plasmid + 100 ng of wild-type ETS1-pCI-neo plasmid (t = 15.7767, p <0.0001), between 200 ng of Tyr149*-mutant ETS1-pCI-neo plasmid and 100 ng of wild-type ETS1-pCI-neo plasmid + 100 ng of Tyr149*-mutant ETS1-pCI-neo plasmid (t = 13.3933, p <0.0001), and between 100 ng of empty pCI-neo plasmid + 100 ng of wild-type ETS1-pCI-neo plasmid and 100 ng of wild-type ETS1-pCI-neo plasmid + 100 ng of Tyr149*-mutant ETS1-pCI-neo plasmid (t = 2.3833, p = 0.4603).
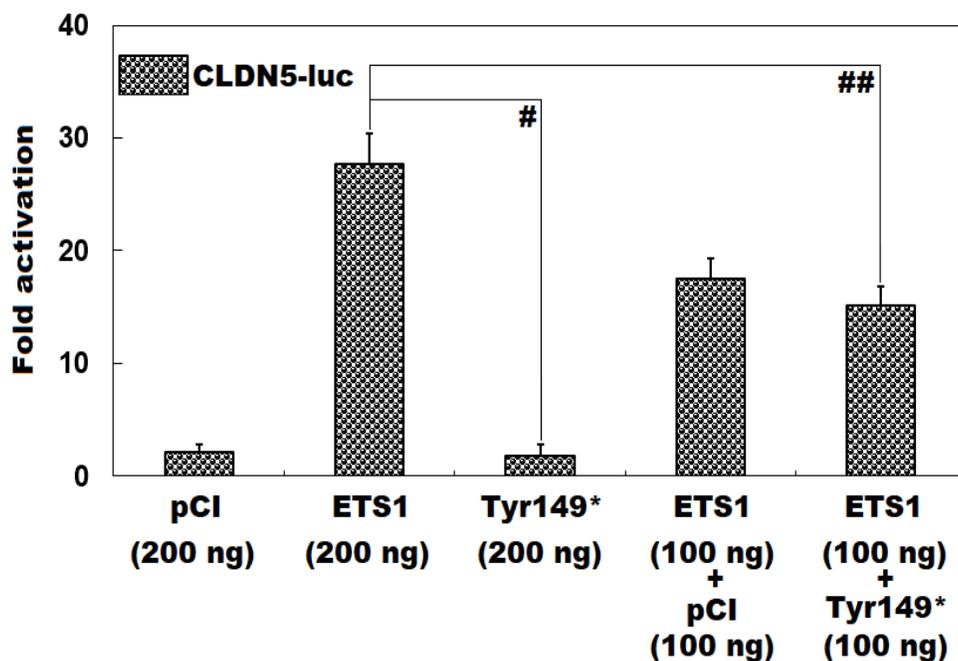

Figure 3. Functional loss of Tyr149*-mutant ETS1 in transactivation of *CLDN5*. A dual-reporter gene assay of the transactivation of the *CLDN5* promoter-induced luciferase expression in cultivated HeLa cells by human wild-type ETS1-pCI-neo (ETS1) or Tyr149*-mutant ETS1-pCI-neo (Tyr149*), alone or in combination, showed that the Tyr149*-mutant ETS1 protein lost transcription activity. For each plasmid utilized, three independent cellular transfections were conducted and analyzed in triplicate. Herein # and ## indicate *p* <0.001 and *p* <0.005.

3.4. Inability of Tyr149-Mutant ETS1 to Transcriptionally Activate ALK1*

As displayed in Figure 4, in HeLa cells routinely cultured in vitro and transiently transfected with various eukaryotic expression plasmids, the wild-type ETS1-pCI-neo plasmid and Tyr149*-mutant ETS1-pCI-neo plasmid induced transcriptional activation of the *ALK1* promoter by ~16-fold and ~1-fold, respectively (Tyr149*-mutant ETS1-pCI-neo vs wild-type ETS1-pCI-neo: t = 11.3841; p = 0.0003). When the wild-type ETS1-pCI-neo and Tyr149*-mutant ETS1-pCI-neo plasmids were co-transfected, the elicited transactivation activity was ~9-fold (wild-type ETS1-pCI-neo vs wild-type ETS1-pCI-neo + Tyr149*-mutant ETS1-pCI-neo: t = 4.9510; p = 0.0078). When multiple-group comparisons were implemented, similar statistical data were obtained (F = 71.745, p = 2.524 × 10^{-7}). Multiple-group comparisons were performed between 200 ng of empty pCI-neo plasmid and 200 ng of wild-type ETS1-pCI-neo plasmid (t = 14.6167, p <0.0001), between 200 ng of empty pCI-neo plasmid and 200 ng of Tyr149*-mutant ETS1-pCI-neo plasmid (t = 0.1333, p = 0.9999), between 200 ng of empty pCI-neo plasmid and 100 ng of empty pCI-neo plasmid + 100 ng of wild-type ETS1-pCI-neo plasmid (t = 8.8067, p <0.0001), between 200 ng of empty pCI-neo plasmid and 100 ng of wild-type ETS1-pCI-neo plasmid + 100 ng of Tyr149*-mutant ETS1-pCI-neo plasmid (t = 7.64, p = 0.0002), between 200 ng of wild-type ETS1-pCI-neo plasmid and 200 ng of Tyr149*-mutant ETS1-pCI-neo plasmid (t = 14.75, p <0.0001), between 200 ng of wild-type ETS1-pCI-neo plasmid and 100 ng of empty pCI-neo plasmid

+ 100 ng of wild-type ETS1-pCI-neo plasmid (t = 5.81, p = 0.0018), between 200 ng of wild-type ETS1-pCI-neo plasmid and 100 ng of wild-type ETS1-pCI-neo plasmid + 100 ng of Tyr149*-mutant ETS1-pCI-neo plasmid (t = 6.9767, p = 0.0004), between 200 ng of Tyr149*-mutant ETS1-pCI-neo plasmid and 100 ng of empty pCI-neo plasmid + 100 ng of wild-type ETS1-pCI-neo plasmid (t = 8.94, p <0.0001), between 200 ng of Tyr149*-mutant ETS1-pCI-neo plasmid and 100 ng of wild-type ETS1-pCI-neo plasmid + 100 ng of Tyr149*-mutant ETS1-pCI-neo plasmid (t = 7.7733, p = 0.0002), and between 100 ng of empty pCI-neo plasmid + 100 ng of wild-type ETS1-pCI-neo plasmid and 100 ng of wild-type ETS1-pCI-neo plasmid + 100 ng of Tyr149*-mutant ETS1-pCI-neo plasmid (t = 1.1667, p = 0.7976).
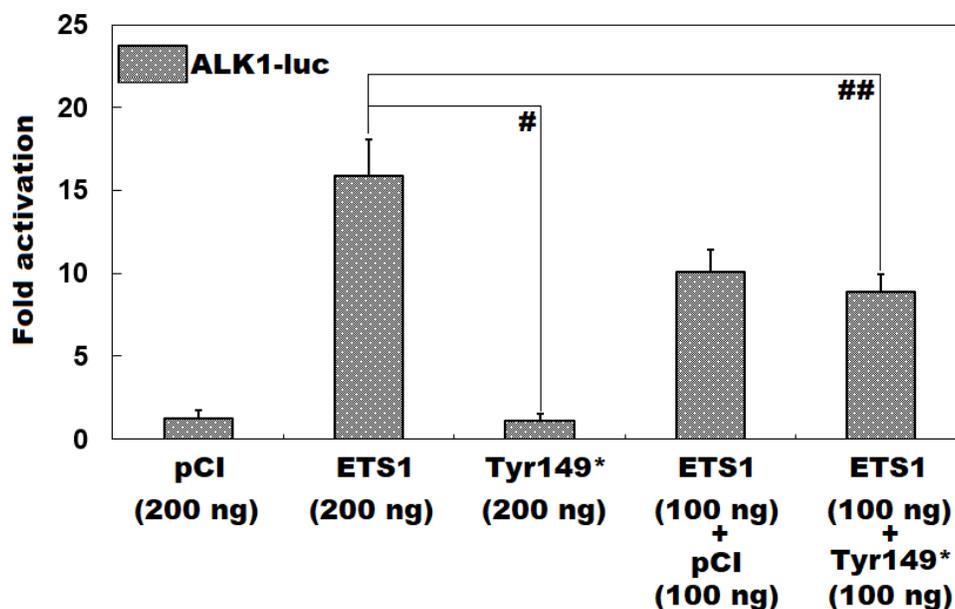

Figure 4. Inability of Tyr149*-mutant ETS1 to transactivate *ALK1*. A dual-reporter gene assay of the transactivation of the *ALK1* promoter-driven luciferase expression in HeLa cells cultured in vitro by human wild-type ETS1-pCI-neo (ETS1) or Tyr149*-mutant ETS1-pCI-neo (Tyr149*), singly or together, unveiled that the Tyr149*-mutant ETS1 protein had no transcriptional function. For each plasmid utilized, three independent cellular transfections were done and assayed in triplicate. Herein # and ## indicate *p* <0.001 and *p* <0.01, respectively.

4. Discussion

In the present investigation, a five-generation pedigree of 42 members affected with DCM was enrolled from the Chinese Han population. By WES-based bioinformatical assay in the available pedigree members, a heterozygous truncating *ETS1* mutation, i.e., NM_005238.4:c.447T>G;p.(Tyr149*), was discovered and verified via a Sanger sequencing assay to co-segregate with DCM in the entire family. This *ETS1* mutation was neither observed in the 552 reference human chromosomes from the Chinese Han population nor found in the population genetics databases of dbSNP and gnomAD. Quantitative biochemical measurement based on dual reporter genes demonstrated that Tyr149*-mutant ETS1 failed to transactivate the expression of *CLDN5* (encoding claudin 5, an integral tight junction protein component) and *ALK1* (coding for activin receptor-like kinase 1), two genes pivotal for proper cardiovascular embryonic development and postnatal structural remodeling [75–85]. These results cumulatively indicate that genetically compromised *ETS1* gives rise to the development of DCM in humans.

In humans, *ETS1* (also known as *ETS-1*, *TPL-1*, *c-ETS-1*, *c-ETS*, *EWSR2*, *P54*, or *ETS*) is mapped on chromosome 11q24.3, containing 8 coding exons and encoding an integral tight junction protein with 441 amino acids, the founding member of the ETS-domain transcription factor family, which is

defined by the existence of an evolutionarily conserved ETS DNA-binding motif that recognizes and binds to the core consensus DNA sequence of GGAA/T (a unique ETS-binding site) in the promoters/enhancers of target genes [86–89]. The ETS family of transcription factors currently comprises 28 members in humans and 27 members in mice, and function as transcriptional regulators (activators or repressors) of numerous downstream target genes that are involved in an extensive assortment of important biological processes including cellular growth, proliferation, differentiation, migration, apoptosis, senescence, and death, hence playing crucial roles in embryonic organogenesis, tissue homeostasis, and the progression of diseases, including arteriosclerosis, autoimmune diseases, allergies, and tumors [86–89]. Although all members of the ETS family share similar protein structures, each member possesses a diverse spectrum of tissue expression and a unique regulatory effect [86–89]. Among the ETS family, ETS1 is characterized by its broad expression, especially by its ample expression in the hearts at all stages from fetuses to adults of humans [90–92] and multiple species of animals [93–98]. Moreover, ETS1 has been validated to have a potent transcriptional regulation function, playing a key role in normal cardiovascular development and postnatal structural remodeling, and in mice, deletion of *Ets1* leads to various cardiovascular developmental abnormalities, including VSD, double-outlet right ventricle (DORV), and ventricular noncompaction [93–97]. ETS1 contains two functionally critical structural domains, including a transcriptional activation domain (TAD) and an ETS domain responsible for recognizing and binding to the promoters/enhancers of target genes [86–89]. In the present research, we identified a novel heterozygous *ETS1* mutation, NM_005238.4:c.447T>G;p.(Tyr149*), to co-segregate with DCM in the whole family. This mutation was anticipated to create a truncated ETS1 protein (Tyr149*), with the entire ETS domain along with a larger part of the TAD domain lost, hence presumably leading to a loss of transcriptional regulation function, which was confirmed by biochemical assays of its two representative target genes, *CLDN5* and *ALK1*. These results support the hypothesis that the haploinsufficiency of *ETS1* predisposes individuals to DCM.

It may be attributed to improper embryonic development and structural remodeling of the heart that *ETS1* haploinsufficiency contributes to DCM. In mice (with a C57BL/6 genetic background), homozygous knockout of *Ets1* led to almost complete perinatal lethality because of profound cardiovascular developmental defects, including a membranous VSD and an anomalous cartilage nodule in the heart [93]. Ye and colleagues [94] reported that in mice (with a C57/B6 background), ETS1 was highly expressed in the cardiac neural crest, endocardium and vascular endothelium early during embryogenesis, and targeted disruption of *Ets1* caused a large membranous VSD and a bifid cardiac apex, as well as a non-apex-forming left ventricle, a hallmark of hypoplastic left heart syndrome (HLHS). Lin et al. [95] reported that deletion of *Ets1* in mice resulted in a cardiovascular developmental defect resembling a DORV in humans. Furthermore, endothelial-specific knockout of *Ets1* in mice led to ventricular noncompaction and coronary vascular developmental anomaly, which reproduced the phenotype caused by global deletion of *Ets1* [96]. Notably, Endothelial-specific ablation of *Ets1* downregulated the expression levels of multiple target genes, including *Alk1* and *Cldn5* [96]. Recently, Nie and Bronner [98] demonstrated that in *Xenopus*, ETS1 was abundantly expressed in the cardiac neural crest and mesoderm during embryogenesis, and knockdown of *Ets1* in the cardiac mesoderm gave rise to an HLHS-like ventricle, which was characteristic of an abundance of cardiomyocytes and a loss of endocardial cells, in line with a key role for ETS1 in mediating cellular fate determination between cardiac myocytes and endocardial cells [97,98]. Zhou and co-workers [99] reported that in the murine embryonic heart, the cardiomyocyte- and endothelial-restricted *Gata4*-occupied genomic regions were enriched for *Ets1* and *Nkx2-5* motifs, respectively, and both ETS1 and NKX2-5 transcription factors interacted with GATA4 to regulate heart development. Of note, both GATA4 and NKX2-5 have been causally linked to human DCM [100–104]. Additionally, in an experimental mouse model with autoimmune myocarditis, treatment with spironolactone (an aldosterone receptor antagonist) significantly alleviated myocardial hypertrophy, improved cardiac function, and diminished myocardial fibrosis via inhibition of ETS1 [105]. In rodent/rat and cellular models with myocardial ischemia/reperfusion (hypoxia/reoxygenation) injury, knockout of *Kdm3a* (coding for

histone demethylase KDM3A) exacerbated myocardial injury and cardiac dysfunction, deteriorated mitochondrial apoptosis and inflammation, and conversely, overexpression of KDM3A could ameliorate such alterations by promoting ETS1 expression [106]. In chicken embryos, copious expression of ETS1 was observed in the heart and endothelial cells of blood vessels [107], and knockdown of *Ets1* hampered the development of the myocardium and coronary system, resulting in a defect in myocardial perfusion [108]. In addition, in cultured ventricular myocytes from chick embryos, ETS1 was shown to transactivate the expression of inducible nitric oxide synthase, presumably via interacting with NF-kappaB [109]. In human embryonic stem cells, ETS1 was identified by single-cell reconstruction of differentiation trajectory to be a pivotal factor responsible for cardiac lineage commitment from a pluripotent status [110]. Taken together, these results highlight the crucial roles of ETS1 in embryonic cardiogenesis and postnatal cardiac remodeling, suggesting that an ETS1 loss-of-function mutation is a molecular defect underlying DCM in humans.

Previously, in humans, chromosome 11q terminal deletions (11q⁻) containing *ETS1* and *ETS1* variations have been implicated in the pathogenesis of Jacobsen syndrome (JS), a rare chromosomal/genetic disorder characterized by a wide spectrum of phenotypes with varying degrees of severity, including congenital heart defects, facial dysmorphisms, intellectual disability, autism and attention deficit, immunodeficiency, genitourinary tract deformities, growth restriction, and thrombocytopenia [111–113]. By comparative genomic hybridization and fluorescence in situ hybridization analyses in five patients from two families with JS, Conrad and partners [111] detected inherited interstitial deletions in the chromosomal region of 11q24.2-q24.3, the smallest ever reported at the JS locus. Specifically, in Family A, a 700-kb interstitial chromosomal deletion of 11q24.3 containing three genes, *ETS1*, *FLI1*, and *SENCR*, was observed; in Family B, a 1.5-Mb interstitial chromosomal deletion of 11q24.2-q24.3 containing eight genes, *ARHGAP32*, *ETS1*, *TP53AIP1*, *FLI1*, *KCNJ1*, *C11orf45*, *SENCR*, and *KCNJ5*, was observed [111]. Of the two JS families, all affected members had *ETS1* haploinsufficiency and manifested such clinical characteristics of JS as developmental malformations (two patients from Family A had minor VSD), immune deficiency, and thrombocytopenia, but had normal cognitive development, consistent with an incomplete penetrance of JS [111]. Grossfeld et al. [112] conducted a prospective study of 110 JS patients with the terminal deletion of chromosome 11q diagnosed by karyotypic analysis, of whom 93 JS patients underwent a comprehensive cardiovascular assessment. As a result, 56% (52/93) of JS patients had severe cardiovascular developmental defects, of which the majority required surgical intervention [112]. In total, two-thirds of the JS patients had a variety of congenital heart defects, including membranous VSD, secundum atrial septal defects, aortic coarctation/stenosis, patent ductus arteriosus, atrioventricular canal defects, mitral valve stenosis, double outlet right ventricle, bicuspid aortic valve, transposition of the great arteries, aberrant right subclavian artery, dextrocardia, a left-sided superior vena cava, and hypoplastic left heart syndrome [112]. By genome-wide single-nucleotide polymorphism array and whole-exome sequencing assays in 538 trios with congenital heart defects, Glessner et al. [113] identified a de novo *ETS1* frameshift variant (c.1044_1049delCAAGGAinsTT or p.Lys349SerfsX2) in one patient with congenital heart malformations (hypoplastic left heart syndrome). Additionally, the integrated data implied that *ETS1* was the causal gene altered by chromosome 11q24.2-q25 deletions in JS [113]. In the current study, a novel *ETS1* loss-of-function variant (c.447T>G or p.Tyr149*) was causally linked to familial DCM, hence expanding the phenotypic spectrum of *ETS1* variations.

5. Conclusions

This investigation unveils *ETS1* as a new gene accountable for DCM in humans, which adds novel insight to the genetic basis of DCM and provides a new molecular target for individualized prophylaxis and treatment of DCM in a subset of patients.

Y.-Q.Y.; performed the experiment, Z.-P.K., J.-N.G., C.-X.Y., X.-L.L., S.Z., Y.-Z.B., Y.-J.X. and Y.-Q.Y.; collecting patients, Z.-P.K., J.-N.G., C.-X.Y., X.-L.L., Y.-J.X. and Y.-Q.Y.; data curation, Z.-P.K. and Y.-Q.Y.; writing—original draft preparation, Z.-P.K., J.-N.G., C.-X.Y., X.-L.L., S.Z., Y.-Z.B., Y.-J.X. and Y.-Q.Y.; writing—review and editing, Z.-P.K. and Y.-Q.Y.; visualization, Z.-P.K. and Y.-Q.Y.; review the final draft, Z.-P.K. and Y.-Q.Y.; supervision, Z.-P.K. and Y.-Q.Y.; project administration, Z.-P.K. and Y.-Q.Y.; funding acquisition, Z.-P.K. All authors have read and agreed to the published version of the manuscript.

Institutional Review Board Statement: This research was completed following the Declaration of Helsinki and approved by the Ethics Committee of Shanghai Fifth People's Hospital, Fudan University (ethical No.: 2020-011).

Informed Consent Statement: Informed consent was provided by all research participants.

Data Availability Statement: The data supporting the discovery of this study are available upon a reasonable request.

Conflicts of Interest: The authors declare no conflict of interest.

References

1. Newman, N.A.; Burke, M.A. Dilated Cardiomyopathy: A Genetic Journey from Past to Future. *Int. J. Mol. Sci.* **2024**, 25, 11460.

2. Eldemire, R.; Mestroni, L.; Taylor, M.R.G. Genetics of Dilated Cardiomyopathy. *Annu. Rev. Med.* **2024**, *75*, 417–426.

3. McGurk, K.A.; Zhang, X.; Theotokis, P.; Thomson, K.; Harper, A.; Buchan, R.J.; Mazaika, E.; Ormondroyd, E.; Wright, W.T.; Macaya, D.; et al. The Penetrance of Rare Variants in Cardiomyopathy-Associated Genes: A Cross-sectional Approach to Estimating Penetrance for Secondary Findings. *Am. J. Hum. Genet.* **2023**, *110*, 1482–1495.

4. Rodríguez-González, E.; Martínez-Legazpi, P.; González-Mansilla, A.; Espinosa, M.Á.; Mombiela, T.; Guzmán De-Villoria, J.A.; Borja, M.G.; Díaz-Otero, F.; Gómez de Antonio, R.; Fernández-García, P.; et al. Cardiac stasis imaging, stroke, and silent brain infarcts in patients with nonischemic dilated cardiomyopathy. *Am. J. Physiol. Heart Circ. Physiol.* **2024**, *327*, H446–H453.

5. Ródenas-Alesina, E.; Lozano-Torres, J.; Tobías-Castillo, P.E.; Badia-Molins, C.; Calvo-Barceló, M.; Vila-Olives, R.; Casas-Masnou, G.; San Emeterio, A.O.; Soriano-Colomé, T.; Fernández-Galera, R.; et al. Risk of Stroke and Incident Atrial Fibrillation in Patients in Sinus Rhythm With Nonischemic Dilated Cardiomyopathy. *Am. J. Cardiol.* **2024**, *233*, 11–18.

6. Fan, Z.; Wu, C.; Wang, C.; Liu, C.; Fang, L.; Ma, L.; Zou, W.; Yuan, B.; Ji, Z.; Cai, B.; et al. Impact of Concurrent Ischaemic Stroke on Unfavourable Outcomes in Men and Women with Dilated Cardiomyopathy. *Rev. Cardiovasc. Med.* **2024**, *25*, 215.

7. Lakdawala, N.K.; Givertz, M.M. Dilated cardiomyopathy with conduction disease and arrhythmia. *Circulation* **2010**, *122*, 527–534.

8. Yuan, Y.; Yang, K.; Liu, Q.; Song, W.; Jin, D.; Zhao, S. Nonspecific intraventricular conduction delay predicts the prognosis of dilated cardiomyopathy. *BMC Cardiovasc. Disord.* **2023**, *23*, 409.

9. Jiménez-Blanco Bravo, M.; Alonso Salinas, G.L.; Parra Esteban, C.; Toquero Ramos, J.; Amores Luque, M.; Zamorano Gómez, J.L.; García-Izquierdo, E.; Álvarez-García, J.; Fernández Lozano, I.; Castro Urda, V. Right Bundle Branch Block Predicts Appropriate Implantable Cardioverter Defibrillator Therapies in Patients with Non-Ischemic Dilated Cardiomyopathy and a Prophylactic Implantable Cardioverter Defibrillator. *Diagnostics* **2024**, *14*, 1173.

10. Raafs, A.G.; Vos, J.L.; Henkens, M.T.H.M.; Verdonschot, J.A.J.; Sikking, M.; Stroeks, S.; Gerretsen, S.; Hazebroek, M.R.; Knackstedt, C.; Nijveldt, R.; et al. Left Atrial Strain Is an Independent Predictor of New-Onset Atrial Fibrillation in Dilated Cardiomyopathy. *JACC Cardiovasc. Imaging* **2023**, *16*, 991–992.

11. Iovănescu, M.L.; Hădăreanu, D.R.; Toader, D.M.; Florescu, C.; Istrătoaie, O.; Donoiu, I.; Militaru, C. The Impact of Atrial Fibrillation on All Heart Chambers Remodeling and Function in Patients with Dilated Cardiomyopathy-A Two- and Three-Dimensional Echocardiography Study. *Life* **2023**, *13*, 1421.

12. Siow, Y.K.; Lin, C.Y.; Chung, F.P.; Lin, Y.J.; Chang, S.L.; Lo, L.W.; Hu, Y.F.; Liao, J.N.; Chang, T.Y.; Tuan, T.C.; et al. Catheter ablation in patients with atrial fibrillation and dilated cardiomyopathy. *Front. Cardiovasc. Med.* **2024**, *11*, 1305485.

13. Zhou, L.; Peng, F.; Li, J.; Gong, H. Exploring novel biomarkers in dilated cardiomyopathy-induced heart failure by integrated analysis and in vitro experiments. *Exp. Ther. Med.* **2023**, *26*, 325.

14. Masè, M.; Rossi, M.; Setti, M.; Barbati, G.; Teso, M.V.; Ribichini, F.L.; Koni, M.; Stolfo, D.; Merlo, M.; Sinagra, G. Applicability and performance of heart failure prognostic scores in dilated cardiomyopathy: the real-world experience of an Italian referral center for cardiomyopathies. *Int. J. Cardiol.* **2024**, *396*, 131562.

15. Hammersley, D.J.; Mukhopadhyay, S.; Chen, X.; Jones, R.E.; Ragavan, A.; Javed, S.; Rajabali, H.; Androulakis, E.; Curran, L.; Mach, L.; et al. Precision prediction of heart failure events in patients with dilated cardiomyopathy and mildly reduced ejection fraction using multi-parametric cardiovascular magnetic resonance. *Eur. J. Heart Fail.* **2024**, *26*, 2553–2562.

16. Tsabedze, N.; du Plessis, A.; Mpanya, D.; Vorster, A.; Wells, Q.; Scholtz, L.; Manga, P. Cardiovascular Magnetic Resonance Imaging Findings in Africans with Idiopathic Dilated Cardiomyopathy. *Diagnostics* **2023**, *13*, 617.

17. Antoniou, N.; Kalaitzoglou, M.; Tsigkriki, L.; Baroutidou, A.; Tsaousidis, A.; Koulaouzidis, G.; Giannakoulas, G.; Charisopoulou, D. Speckle Tracking Echocardiography in Patients with Non-Ischemic Dilated Cardiomyopathy Who Undergo Cardiac Resynchronization Therapy: A Narrative Review. *Diagnostics* **2024**, *14*, 1178.

18. Winiarczyk, M.; Dziewięcka, E.; Wiśniowska-Śmiałek, S.; Stępień, A.; Graczyk, K.; Leśniak-Sobelga, A.; Hlawaty, M.; Woźniak, J.; Savitskaya, M.; Holcman, K.; et al. Left ventricular diastolic dysfunction worsens prognosis in patients with heart failure due to dilated cardiomyopathy. *ESC Heart Fail.* **2025**, *12*, 1183–1193.

19. Kimura, Y.; Beukers, H.K.C.; Rademaker, R.; Chen, H.S.; Ebert, M.; Jensen, T.; Piers, S.R.; Wijnmaalen, A.P.; de Riva, M.; Dekkers, O.M.; et al. Volume-Weighted Unipolar Voltage Predicts Heart Failure Mortality in Patients With Dilated Cardiomyopathy and Ventricular Arrhythmias. *JACC Clin. Electrophysiol.* **2023**, *9*, 965–975.

20. Ma, H.Y.; Xie, G.Y.; Tao, J.; Li, Z.Z.; Liu, P.; Zheng, X.J.; Wang, R.P. Identification of patients with nonischemic dilated cardiomyopathy at risk of malignant ventricular arrhythmias: insights from cardiac magnetic resonance feature tracking. *BMC Cardiovasc. Disord.* **2024**, *24*, 29.

21. Amyar, A.; Al-Deiri, D.; Sroubek, J.; Kiang, A.; Ghanbari, F.; Nakamori, S.; Rodriguez, J.; Kramer, D.B.; Manning, W.J.; Kwon, D.; et al. Radiomic Cardiac MRI Signatures for Predicting Ventricular Arrhythmias in Patients With Nonischemic Dilated Cardiomyopathy. *JACC Adv.* **2025**, *4*, 101684.

22. Li, Y.; Xu, Y.; Li, W.; Guo, J.; Wan, K.; Wang, J.; Xu, Z.; Han, Y.; Sun, J.; Chen, Y. Cardiac MRI to Predict Sudden Cardiac Death Risk in Dilated Cardiomyopathy. *Radiology* **2023**, *307*, e222552.

23. Kantor, P.F.; Shi, L.; Colan, S.D.; Orav, E.J.; Wilkinson, J.D.; Hamza, T.H.; Webber, S.A.; Canter, C.E.; Towbin, J.A.; Everitt, M.D.; et al. Progressive Left Ventricular Remodeling for Predicting Mortality in Children With Dilated Cardiomyopathy: The Pediatric Cardiomyopathy Registry. *J. Am. Heart Assoc.* **2024**, *13*, e022557.

24. Street-de Palma, C.; Lim, Z.; Field, E.; Kaski, J.P.; Norrish, G. Imaging based risk factors for heart failure death in childhood dilated cardiomyopathy: a systematic review and meta-analysis. *Front. Cardiovasc. Med.* **2025**, *12*, 1568494.

25. Wang, S.; Zhang, Z.; He, J.; Liu, J.; Guo, X.; Chu, H.; Xu, H.; Wang, Y. Comprehensive review on gene mutations contributing to dilated cardiomyopathy. *Front. Cardiovasc. Med.* **2023**, *10*, 1296389.

26. Alexander, P.M.; Daubeney, P.E.; Nugent, A.W.; Lee, K.J.; Turner, C.; Colan, S.D.; Robertson, T.; Davis, A.M.; Ramsay, J.; Justo, R.; et al. Long-term outcomes of dilated cardiomyopathy diagnosed during childhood: results from a national population-based study of childhood cardiomyopathy. *Circulation* **2013**, *128*, 2039–2046.

27. Hammersley, D.J.; Jones, R.E.; Owen, R.; Mach, L.; Lota, A.S.; Khalique, Z.; De Marvao, A.; Androulakis, E.; Hatipoglu, S.; Gulati, A.; et al. Phenotype, Outcomes and Natural History of Early-Stage Non-Ischaemic Cardiomyopathy. *Eur. J. Heart Fail.* **2023**, *25*, 2050–2059.

28. Merlo, M.; Cannatà, A.; Pio Loco, C.; Stolfo, D.; Barbati, G.; Artico, J.; Gentile, P.; De Paris, V.; Ramani, F.; Zecchin, M.; et al. Contemporary Survival Trends and Etiological Characterization in Non-Ischemic Dilated Cardiomyopathy. *Eur. J. Heart Fail.* **2020**, *22*, 1111–1121.

29. Kadhi, A.; Mohammed, F.; Nemer, G. The Genetic Pathways Underlying Immunotherapy in Dilated Cardiomyopathy. *Front. Cardiovasc. Med.* **2021**, *8*, 613295.

30. Lv, Y.; Gao, R.F.; Yang, C.X.; Xu, Y.J.; Yang, Y.Q. Increased gestational palmitic acid predisposes offspring to congenital heart disease. *Cell Rep. Med.* **2023**, *4*, 100984.

31. Peters, S.A.; Wright, L.; Yao, J.; McCall, L.; Thompson, T.; Thompson, B.; Johnson, R.; Huynh, Q.; Santiago, C.F.; Trainer, A.; et al. Environmental Risk Factors Are Associated With the Natural History of Familial Dilated Cardiomyopathy. *J. Am. Heart Assoc.* **2025**, *14*, e037311.

32. Tsabedze, N.; Ramsay, M.; Krause, A.; Wells, Q.; Mpanya, D.; Manga, P. The genetic basis for adult-onset idiopathic dilated cardiomyopathy in people of African descent. *Heart Fail. Rev.* **2023**, *28*, 879–892.

33. Chun, Y.W.; Miyamoto, M.; Williams, C.H.; Neitzel, L.R.; Silver-Isenstadt, M.; Cadar, A.G.; Fuller, D.T.; Fong, D.C.; Liu, H.; Lease, R.; et al. Impaired Reorganization of Centrosome Structure Underlies Human Infantile Dilated Cardiomyopathy. *Circulation* **2023**, *147*, 1291–1303.

34. Hofmeyer, M.; Haas, G.J.; Jordan, E.; Cao, J.; Kransdorf, E.; Ewald, G.A.; Morris, A.A.; Owens, A.; Lowes, B.; Stoller, D.; et al. Rare Variant Genetics and Dilated Cardiomyopathy Severity: The DCM Precision Medicine Study. *Circulation* **2023**, *148*, 872–881.

35. Stroeks, S.L.V.M.; Lunde, I.G.; Hellebrekers, D.M.E.I.; Claes, G.R.F.; Wakimoto, H.; Gorham, J.; Krapels, I.P.C.; Vanhoutte, E.K.; van den Wijngaard, A.; Henkens, M.T.H.M.; et al. Prevalence and Clinical Consequences of Multiple Pathogenic Variants in Dilated Cardiomyopathy. *Circ. Genom. Precis. Med.* **2023**, *16*, e003788.

36. Johnson, R.; Otway, R.; Chin, E.; Horvat, C.; Ohanian, M.; Wilcox, J.A.L.; Su, Z.; Prestes, P.; Smolnikov, A.; Soka, M.; et al. DMD-Associated Dilated Cardiomyopathy: Genotypes, Phenotypes, and Phenocopies. *Circ. Genom. Precis. Med.* **2023**, *16*, 421-430.

37. Gu, J.N.; Yang, C.X.; Ding, Y.Y.; Qiao, Q.; Di, R.M.; Sun, Y.M.; Wang, J.; Yang, L.; Xu, Y.J.; Yang, Y.Q. Identification of BMP10 as a Novel Gene Contributing to Dilated Cardiomyopathy. *Diagnostics* **2023**, *13*, 242.

38. Bertero, E.; Fracasso, G.; Eustachi, V.; Coviello, D.; Cecconi, M.; Giovinazzo, S.; Toma, M.; Merlo, M.; Sinagra, G.; Porto, I.; et al. Diagnostic yield and predictive value on left ventricular remodelling of genetic testing in dilated cardiomyopathy. *ESC Heart Fail.* **2023**, *10*, 2745–2750.

39. Sono, R.; Larrinaga, T.M.; Huang, A.; Makhlouf, F.; Kang, X.; Su, J.; Lau, R.; Arboleda, V.A.; Biniwale, R.; Fishbein, G.A.; et al. Whole-Exome Sequencing Identifies Homozygote Nonsense Variants in LMOD2 Gene Causing Infantile Dilated Cardiomyopathy. *Cells* **2023**, *12*, 1455.

40. Lian, H.; Song, S.; Chen, W.; Shi, A.; Jiang, H.; Hu, S. Genetic characterization of dilated cardiomyopathy patients undergoing heart transplantation in the Chinese population by whole-exome sequencing. *J. Transl. Med.* **2023**, *21*, 476.

41. Yu, T.; Yan, F.; Xu, Y.; Hunag, Y.; Gong, H.; Zhao, P.; Sun, D.; Zhang, Y.; Zhang, F.; He, X. Identification of a novel TNNI3 synonymous variant causing intron retention in autosomal recessive dilated cardiomyopathy. *Gene* **2023**, *856*, 147102.

42. Shi, H.Y.; Xie, M.S.; Guo, Y.H.; Yang, C.X.; Gu, J.N.; Qiao, Q.; Di, R.M.; Qiu, X.B.; Xu, Y.J.; Yang, Y.Q. VEZF1 loss-of-function mutation underlying familial dilated cardiomyopathy. *Eur. J. Med. Genet.* **2023**, *66*, 104705.

43. Ghasemi, S.; Mahdavi, M.; Maleki, M.; Salahshourifar, I.; Kalayinia, S. Novel pathogenic variant in MED12 causing non-syndromic dilated cardiomyopathy. *BMC Med. Genomics* **2023**, *16*, 334.

44. Zheng, S.L.; Henry, A.; Cannie, D.; Lee, M.; Miller, D.; McGurk, K.A.; Bond, I.; Xu, X.; Issa, H.; Francis, C.; et al. Genome-wide association analysis provides insights into the molecular etiology of dilated cardiomyopathy. *Nat. Genet.* **2024**, *56*, 2646–2658.

45. Jurgens, S.J.; Rämö, J.T.; Kramarenko, D.R.; Wijdeveld, L.F.J.M.; Haas, J.; Chaffin, M.D.; Garnier, S.; Gaziano, L.; Weng, L.C.; Lipov, A.; et al. Genome-wide association study reveals mechanisms underlying dilated cardiomyopathy and myocardial resilience. *Nat. Genet.* **2024**, *56*, 2636–2645.

46. Li, Y.; Ma, K.; Dong, Z.; Gao, S.; Zhang, J.; Huang, S.; Yang, J.; Fang, G.; Li, Y.; Li, X.; et al. Frameshift variants in C10orf71 cause dilated cardiomyopathy in human, mouse, and organoid models. *J. Clin. Invest.* **2024**, *134*, e177172.

47. Amor-Salamanca, A.; Santana Rodríguez, A.; Rasoul, H.; Rodríguez-Palomares, J.F.; Moldovan, O.; Hey, T.M.; Delgado, M.G.; Cuenca, D.L.; de Castro Campos, D.; Basurte-Elorz, M.T.; et al. Role of TBX20 Truncating Variants in Dilated Cardiomyopathy and Left Ventricular Noncompaction. *Circ. Genom. Precis. Med.* **2024**, *17*, e004404.

48. Gao, X.; Pang, S.; Ding, L.; Yan, H.; Cui, Y.; Yan, B. Genetic and functional variants of the TBX20 gene promoter in dilated cardiomyopathy. *Mol. Genet. Genomic Med.* **2024**, *12*, e2355.

49. de Frutos, F.; Ochoa, J.P.; Webster, G.; Jansen, M.; Remior, P.; Rasmussen, T.B.; Sabater-Molina, M.; Barriales-Villa, R.; Girolami, F.; Cesar, S.; et al. Clinical Features and Outcomes of Pediatric MYH7-Related Dilated Cardiomyopathy. *J. Am. Heart Assoc.* **2024**, *13*, e036208.

50. Kraoua, L.; Louati, A.; Ahmed, S.B.; Abida, N.; Khemiri, M.; Menif, K.; Mrad, R.; Zaffran, S.; Jaouadi, H. Homozygous TNNI3 frameshift variant in a consanguineous family with lethal infantile dilated cardiomyopathy. *Mol. Genet. Genomic Med.* **2024**, *12*, e2486.

51. Ochoa, J.P.; Lalaguna, L.; Mirelis, J.G.; Dominguez, F.; Gonzalez-Lopez, E.; Salas, C.; Roustan, G.; McGurk, K.A.; Zheng, S.L.; Barton, P.J.R.; et al. Biallelic Loss of Function Variants in Myocardial Zonula Adherens Protein Gene (MYZAP) Cause a Severe Recessive Form of Dilated Cardiomyopathy. *Circ. Heart Fail.* **2024**, *17*, e011226.

52. Ha, C.; Kim, D.; Bak, M.; Park, J.H.; Kim, Y.G.; Jang, J.H.; Kim, J.W.; Choi, J.O.; Jang, M.A. CRYAB stop-loss variant causes rare syndromic dilated cardiomyopathy with congenital cataract: expanding the phenotypic and mutational spectrum of alpha-B crystallinopathy. *J. Hum. Genet.* **2024**, *69*, 159–162.

53. Perret, C.; Proust, C.; Esslinger, U.; Ader, F.; Haas, J.; Pruny, J.F.; Isnard, R.; Richard, P.; Trégouët, D.A.; Charron, P.; et al. DNA-pools targeted-sequencing as a robust cost-effective method to detect rare variants: Application to dilated cardiomyopathy genetic diagnosis. *Clin. Genet.* **2024**, *105*, 185–189.

54. Tran, D.D.; Lien, N.T.K.; Tung, N.V.; Huu, N.C.; Nguyen, P.T.; Tien, D.A.; Thu, D.T.H.; Huy, B.Q.; Oanh, T.T.K.; Lien, N.T.P.; et al. Three Novel Pathogenic Variants in Unrelated Vietnamese Patients with Cardiomyopathy. *Diagnostics* **2024**, *14*, 2709.

55. Voinescu, O.R.; Ionescu, B.I.; Militaru, S.; Afana, A.S.; Sascau, R.; Vasiliu, L.; Onciul, S.; Dobrescu, M.A.; Cozlac, R.A.; Cozma, D.; et al. Genetic Characterization of Dilated Cardiomyopathy in Romanian Adult Patients. *Int. J. Mol. Sci.* **2024**, *25*, 2562.

56. d'Apolito, M.; Ranaldi, A.; Santoro, F.; Cannito, S.; Gravina, M.; Santacroce, R.; Ragnatela, I.; Margaglione, A.; D'Andrea, G.; Casavecchia, G.; et al. De Novo p.Asp3368Gly Variant of Dystrophin Gene Associated with X-Linked Dilated Cardiomyopathy and Skeletal Myopathy: Clinical Features and In Silico Analysis. *Int. J. Mol. Sci.* **2024**, *25*, 2787.

57. Mozafary Bazargany, M.; Esmaeili, S.; Hesami, M.; Houshmand, G.; Mahdavi, M.; Maleki, M.; Kalayinia, S. A novel likely pathogenic homozygous RBCK1 variant in dilated cardiomyopathy with muscle weakness. *ESC Heart Fail.* **2024**, *11*, 1472–1482.

58. Kubanek, M.; Binova, J.; Piherova, L.; Krebsova, A.; Kotrc, M.; Hartmannova, H.; Hodanova, K.; Musalkova, D.; Stranecky, V.; Palecek, T.; et al. Genotype is associated with left ventricular reverse remodelling and early events in recent-onset dilated cardiomyopathy. *ESC Heart Fail.* **2024**, *11*, 4127–4138.

59. León, P.; Franco, P.; Hinojosa, N.; Torres, K.; Moreano, A.; Romero, V.I. TTN novel splice variant in familial dilated cardiomyopathy and splice variants review: a case report. *Front. Cardiovasc. Med.* **2024**, *11*, 1387063.

60. Carigi, S.; Olivucci, G.; Cristalli, C.P.; Marzo, F.; Isidori, F.; Palmieri, S.; Schiavo, M.A.; Gualandi, F.; Amati, S.; Rocchetti, L.M.; et al. A single RBM20 missense variant is a potential contributor to dilated cardiomyopathy and/or isolated left ventricular dilatation in the Emilia Romagna region of Italy. *Int. J. Cardiol.* **2025**, *423*, 132999.

61. Jadidi, M.; Babaali, V.; InanlooRahatloo, K.; Salehi, N.; Mollazadeh, R. Identification of a rare variant in TNNT3 responsible for familial dilated cardiomyopathy through whole-exome sequencing and in silico analysis. *Eur. J. Med. Res.* **2025**, *30*, 424.

62. Jiang, W.F.; Sun, Y.M.; Qiu, X.B.; Wu, S.H.; Ding, Y.Y.; Li, N.; Yang, C.X.; Xu, Y.J.; Jiang, T.B.; Yang, Y.Q. Identification and Functional Investigation of *SOX4* as a Novel Gene Underpinning Familial Atrial Fibrillation. *Diagnostics* **2024**, *14*, 2376.

63. Li, Y.J.; Wang, J.; Ye, W.G.; Liu, X.Y.; Li, L.; Qiu, X.B.; Chen, H.; Xu, Y.J.; Yang, Y.Q.; Bai, D.; et al. Discovery of *GJC1* (Cx45) as a New Gene Underlying Congenital Heart Disease and Arrhythmias. *Biology* **2023**, *12*, 346.

64. Li, N.; Li, Y.J.; Guo, X.J.; Wu, S.H.; Jiang, W.F.; Zhang, D.L.; Wang, K.W.; Li, L.; Sun, Y.M.; Xu, Y.J.; et al. Discovery of TBX20 as a Novel Gene Underlying Atrial Fibrillation. *Biology* **2023**, *12*, 1186.

65. Cho, J.; Kim, J.; Song, J.S.; Uh, Y.; Lee, J.H.; Lee, H.S. Whole-Exome Sequencing and Analysis of the T Cell Receptor β and γ Repertoires in Rheumatoid Arthritis. *Diagnostics* **2024**, *14*, 529.

66. Fang, H.H.; Lee, C.L.; Chen, H.J.; Chuang, C.K.; Chiu, H.C.; Chang, Y.H.; Tu, Y.R.; Lo, Y.T.; Lin, H.Y.; Lin, S.P. Whole Exome Sequencing Facilitates Early Diagnosis of Lesch-Nyhan Syndrome: A Case Series. *Diagnostics* **2024**, *14*, 2809.

67. Li, H.; Durbin, R. Fast and accurate short read alignment with Burrows–Wheeler transform. *Bioinformatics* **2009**, *25*, 1754–1760.

68. McKenna, A.; Hanna, M.; Banks, E.; Sivachenko, A.; Cibulskis, K.; Kernytsky, A.; Garimella, K.; Altshuler, D.; Gabriel, S.; Daly, M. The Genome Analysis Toolkit: A MapReduce framework for analyzing next-generation DNA sequencing data. *Genome Res.* **2010**, *20*, 1297–1303.

69. Wang, K.; Li, M.; Hakonarson, H. ANNOVAR: functional annotation of genetic variants from high-throughput sequencing data. *Nucleic Acids Res.* **2010**, *38*, e164.

70. Wang, Z.; Liu, X.Y.; Yang, C.X.; Zhou, H.M.; Li, Y.J.; Qiu, X.B.; Huang, R.T.; Cen, S.S.; Wang, Y.; Xu, Y.J.; et al. Discovery and functional investigation of BMP4 as a new causative gene for human congenital heart disease. *Am. J. Transl. Res.* **2024**, *16*, 2034–2048.

71. Abhinav, P.; Li, Y.J.; Huang, R.T.; Liu, X.Y.; Gu, J.N.; Yang, C.X.; Xu, Y.J.; Wang, J.; Yang, Y.Q. Somatic GATA4 mutation contributes to tetralogy of Fallot. *Exp. Ther. Med.* **2024**, *27*, 91.

72. Li, Y.J.; Zou, S.; Bian, Y.Z.; Liu, X.Y.; Yang, C.X.; Li, L.; Qiu, X.B.; Xu, Y.J.; Yang, Y.Q.; Huang, R.T. Chromosomal Location and Identification of TBX20 as a New Gene Responsible for Familial Bicuspid Aortic Valve. *Diagnostics* **2025**, *15*, 600.

73. Dong, B.B.; Li, Y.J.; Liu, X.Y.; Huang, R.T.; Yang, C.X.; Xu, Y.J.; Lv, H.T.; Yang, Y.Q. Discovery of BMP10 as a new gene underpinning congenital heart defects. *Am. J. Transl. Res.* **2024**, *16*, 109–125.

74. Yan, Z.; Dong, B.B.; Li, Y.J.; Yang, C.X.; Xu, Y.J.; Huang, R.T.; Liu, X.Y.; Yang, Y.Q. Identification and Functional Characterization of a Novel SOX4 Mutation Predisposing to Coffin-Siris Syndromic Congenital Heart Disease. *Children* **2025**, *12*, 608.

75. Jiang, S.; Liu, S.; Hou, Y.; Lu, C.; Yang, W.; Ji, T.; Yang, Y.; Yu, Z.; Jin, Z. Cardiac-specific overexpression of Claudin-5 exerts protection against myocardial ischemia and reperfusion injury. *Biochim. Biophys. Acta Mol. Basis Dis.* **2022**, *1868*, 166535.

76. Zhang, Y.; Chen, B.; Wang, M.; Liu, H.; Chen, M.; Zhu, J.; Zhang, Y.; Wang, X.; Wu, Y.; Liu, D.; et al. A novel function of claudin-5 in maintaining the structural integrity of the heart and its implications in cardiac pathology. *Biochim. Biophys. Acta Mol. Basis Dis.* **2024**, *1870*, 167274.

77. Burek, M.; Arias-Loza, P.A.; Roewer, N.; Förster, C.Y. Claudin-5 as a novel estrogen target in vascular endothelium. *Arterioscler. Thromb. Vasc. Biol.* **2010**, *30*, 298–304.

78. Sanford, J.L.; Edwards, J.D.; Mays, T.A.; Gong, B.; Merriam, A.P.; Rafael-Fortney, J.A. Claudin-5 localizes to the lateral membranes of cardiomyocytes and is altered in utrophin/dystrophin-deficient cardiomyopathic mice. *J. Mol. Cell. Cardiol.* **2005**, *38*, 323-332.

79. Milani-Nejad, N.; Schultz, E.J.; Slabaugh, J.L.; Janssen, P.M.; Rafael-Fortney, J.A. Myocardial Contractile Dysfunction Is Present without Histopathology in a Mouse Model of Limb-Girdle Muscular Dystrophy-2F and Is Prevented after Claudin-5 Virotherapy. *Front. Physiol.* **2016**, *7*, 539.

80. Delfín, D.A.; Xu, Y.; Schill, K.E.; Mays, T.A.; Canan, B.D.; Zang, K.E.; Barnum, J.A.; Janssen, P.M.; Rafael-Fortney, J.A. Sustaining cardiac claudin-5 levels prevents functional hallmarks of cardiomyopathy in a muscular dystrophy mouse model. *Mol. Ther.* **2012**, *20*, 1378–1383.

81. Luo, T.; Liu, H.; Chen, B.; Liu, H.; Abdel-Latif, A.; Kitakaze, M.; Wang, X.; Wu, Y.; Chou, D.; Kim, J.K. A Novel Role of Claudin-5 in Prevention of Mitochondrial Fission Against Ischemic/Hypoxic Stress in Cardiomyocytes. *Can. J. Cardiol.* **2021**, *37*, 1593–1606.

82. Mays, T.A.; Binkley, P.F.; Lesinski, A.; Doshi, A.A.; Quaile, M.P.; Margulies, K.B.; Janssen, P.M.; Rafael-Fortney, J.A. Claudin-5 levels are reduced in human end-stage cardiomyopathy. *J. Mol. Cell. Cardiol.* **2008**, *45*, 81–87.

83. Swager, S.A.; Delfín, D.A.; Rastogi, N.; Wang, H.; Canan, B.D.; Fedorov, V.V.; Mohler, P.J.; Kilic, A.; Higgins, R.S.D.; Ziolo, M.T.; et al. Claudin-5 levels are reduced from multiple cell types in human failing hearts and are associated with mislocalization of ephrin-B1. *Cardiovasc. Pathol.* **2015**, *24*, 160–167.

84. Capasso, T.L.; Li, B.; Volek, H.J.; Khalid, W.; Rochon, E.R.; Anbalagan, A.; Herdman, C.; Yost, H.J.; Villanueva, F.S.; Kim, K.; et al. BMP10-mediated ALK1 signaling is continuously required for vascular development and maintenance. *Angiogenesis* **2020**, *23*, 203–220.

85. Bhave, S.; Swain, L.; Qiao, X.; Martin, G.; Aryaputra, T.; Everett, K.; Kapur, N.K. ALK1 Deficiency Impairs the Wound-Healing Process and Increases Mortality in Murine Model of Myocardial Infarction. *J. Cardiovasc. Transl. Res.* **2024**, *17*, 496–504.

86. Garrett-Sinha, L.A. Review of Ets1 structure, function, and roles in immunity. *Cell. Mol. Life Sci.* **2013**, *70*, 3375–3390.

87. Shiu, Y.T.; Jaimes, E.A. Transcription Factor ETS-1 and Reactive Oxygen Species: Role in Vascular and Renal Injury. *Antioxidants* **2018**, *7*, 84.

88. Yang, Y.; Han, X.; Sun, L.; Shao, F.; Yin, Y.; Zhang, W. ETS Transcription Factors in Immune Cells and Immune-Related Diseases. *Int. J. Mol. Sci.* **2024**, *25*, 10004.

89. Wang, S.; Wan, L.; Zhang, X.; Fang, H.; Zhang, M.; Li, F.; Yan, D. ETS-1 in tumor immunology: implications for novel anti-cancer strategies. *Front. Immunol.* **2025**, *16*, 1526368.

90. Szabo, L.; Morey, R.; Palpant, N.J.; Wang, P.L.; Afari, N.; Jiang, C.; Parast, M.M.; Murry, C.E.; Laurent, L.C.; Salzman, J. Statistically based splicing detection reveals neural enrichment and tissue-specific induction of circular RNA during human fetal development. *Genome Biol.* **2015**, *16*, 126.

91. Duff, M.O.; Olson, S.; Wei, X.; Garrett, S.C.; Osman, A.; Bolisetty, M.; Plocik, A.; Celniker, S.E.; Graveley, B.R. Genome-wide identification of zero nucleotide recursive splicing in Drosophila. *Nature* **2015**, *521*, 376–379.

92. Fagerberg, L.; Hallström, B.M.; Oksvold, P.; Kampf, C.; Djureinovic, D.; Odeberg, J.; Habuka, M.; Tahmasebpoor, S.; Danielsson, A.; Edlund, K.; et al. Analysis of the human tissue-specific expression by genome-wide integration of transcriptomics and antibody-based proteomics. *Mol. Cell. Proteomics* **2014**, *13*, 397–406.

93. Gao, Z.; Kim, G.H.; Mackinnon, A.C.; Flagg, A.E.; Bassett, B.; Earley, J.U.; Svensson, E.C. Ets1 is required for proper migration and differentiation of the cardiac neural crest. *Development* **2010**, *137*, 1543–1551.

94. Ye, M.; Coldren, C.; Benson, W.; Goldmuntz, E.; Ostrowski, M.; Watson, D.; Perryman, B.; Grossfeld, P. Deletion of *ETS-1*, a gene in the Jacobsen syndrome critical region, causes ventricular septal defects and abnormal ventricular morphology in mice. *Hum. Mol. Genet.* **2010**, *19*, 648–656.

95. Lin, L.; Pinto, A.; Wang, L.; Fukatsu, K.; Yin, Y.; Bamforth, S.D.; Bronner, M.E.; Evans, S.M.; Nie, S.; Anderson, R.H.; et al. ETS1 loss in mice impairs cardiac outflow tract septation via a cell migration defect autonomous to the neural crest. *Hum. Mol. Genet.* **2022**, *31*, 4217–4227.

96. Wang, L.; Lin, L.; Qi, H.; Chen, J.; Grossfeld, P. Endothelial Loss of ETS1 Impairs Coronary Vascular Development and Leads to Ventricular Non-Compaction. *Circ. Res.* **2022**, *131*, 371–387.

97. Grossfeld, P. ETS1 and HLHS: Implications for the Role of the Endocardium. *J. Cardiovasc. Dev. Dis.* **2022**, *9*, 219.

98. Nie, S.; Bronner, M.E. Dual developmental role of transcriptional regulator Ets1 in Xenopus cardiac neural crest vs. heart mesoderm. *Cardiovasc. Res.* **2015**, *106*, 67–75.

99. Zhou, P.; Zhang, Y.; Sethi, I.; Ye, L.; Trembley, M.A.; Cao, Y.; Akerberg, B.N.; Xiao, F.; Zhang, X.; Li, K.; et al. GATA4 Regulates Developing Endocardium Through Interaction With ETS1. *Circ. Res.* **2022**, *131*, e152–e168.

100. Zhao, L.; Xu, J.H.; Xu, W.J.; Yu, H.; Wang, Q.; Zheng, H.Z.; Jiang, W.F.; Jiang, J.F.; Yang, Y.Q. A novel GATA4 loss-of-function mutation responsible for familial dilated cardiomyopathy. *Int. J. Mol. Med.* **2014**, *33*, 654–660.

101. Li, J.; Liu, W.D.; Yang, Z.L.; Yuan, F.; Xu, L.; Li, R.G.; Yang, Y.Q. Prevalence and spectrum of GATA4 mutations associated with sporadic dilated cardiomyopathy. *Gene* **2014**, *548*, 174–181.

102. Costa, M.W.; Guo, G.; Wolstein, O.; Vale, M.; Castro, M.L.; Wang, L.; Otway, R.; Riek, P.; Cochrane, N.; Furtado, M.; et al. Functional characterization of a novel mutation in NKX2-5 associated with congenital heart disease and adult-onset cardiomyopathy. *Circ. Cardiovasc. Genet.* **2013**, *6*, 238–247.

103. Yuan, F.; Qiu, X.B.; Li, R.G.; Qu, X.K.; Wang, J.; Xu, Y.J.; Liu, X.; Fang, W.Y.; Yang, Y.Q.; Liao, D.N. A novel NKX2-5 loss-of-function mutation predisposes to familial dilated cardiomyopathy and arrhythmias. *Int. J. Mol. Med.* **2015**, *35*, 478–486.

104. Sveinbjornsson, G.; Olafsdottir, E.F.; Thorolfsdottir, R.B.; Davidsson, O.B.; Helgadottir, A.; Jonasdottir, A.; Jonasdottir, A.; Bjornsson, E.; Jensson, B.O.; Arnadottir, G.A.; et al. Variants in NKX2-5 and FLNC Cause Dilated Cardiomyopathy and Sudden Cardiac Death. *Circ. Genom. Precis. Med.* **2018**, *11*, e002151.

105. Wang, W.K.; Wang, B.; Cao, X.H.; Liu, Y.S. Spironolactone alleviates myocardial fibrosis via inhibition of Ets-1 in mice with experimental autoimmune myocarditis. *Exp. Ther. Med.* **2022**, *23*, 369.

106. Guo, X.; Zhang, B.F.; Zhang, J.; Liu, G.; Hu, Q.; Chen, J. The histone demthylase KDM3A protects the myocardium from ischemia/reperfusion injury via promotion of ETS1 expression. *Commun. Biol.* **2022**, *5*, 270.

107. Tahtakran, S.A.; Selleck, M.A. Ets-1 expression is associated with cranial neural crest migration and vasculogenesis in the chick embryo. *Gene Expr. Patterns* **2003**, *3*, 455–458.

108. Lie-Venema, H.; Gittenberger-de Groot, A.C.; van Empel, L.J.; Boot, M.J.; Kerkdijk, H.; de Kant, E.; DeRuiter, M.C. Ets-1 and Ets-2 transcription factors are essential for normal coronary and myocardial development in chicken embryos. *Circ. Res.* **2003**, *92*, 749–756.

109. Takahashi, T.; Sugishita, Y.; Kinugawa, K.; Shimizu, T.; Yao, A.; Harada, K.; Matsui, H.; Nagai, R. Ets-1 is involved in transcriptional regulation of the chick inducible nitric oxide synthase gene in embryonic ventricular myocytes. *Mol. Cell. Biochem.* **2001**, *226*, 57–65.

110. Ruan, H.; Liao, Y.; Ren, Z.; Mao, L.; Yao, F.; Yu, P.; Ye, Y.; Zhang, Z.; Li, S.; Xu, H.; et al. Single-cell reconstruction of differentiation trajectory reveals a critical role of ETS1 in human cardiac lineage commitment. *BMC Biol.* **2019**, *17*, 89.

111. Conrad, S.; Demurger, F.; Moradkhani, K.; Pichon, O.; Le Caignec, C.; Pascal, C.; Thomas, C.; Bayart, S.; Perlat, A.; Dubourg, C.; et al. 11q24.2q24.3 microdeletion in two families presenting features of Jacobsen syndrome, without intellectual disability: Role of FLI1, ETS1, and SENCR long noncoding RNA. *Am. J. Med. Genet. A* **2019**, *179*, 993–1000.

112. Grossfeld, P.D.; Mattina, T.; Lai, Z.; Favier, R.; Jones, K.L.; Cotter, F.; Jones, C. The 11q terminal deletion disorder: A prospective study of 110 cases. *Am. J. Med. Genet. A* **2004**, *129A*, 51–61.

113. Glessner, J.T.; Bick, A.G.; Ito, K.; Homsy, J.; Rodriguez-Murillo, L.; Fromer, M.; Mazaika, E.; Vardarajan, B.; Italia, M.; Leipzig, J.; et al. Increased frequency of de novo copy number variants in congenital heart disease by integrative analysis of single nucleotide polymorphism array and exome sequence data. *Circ. Res.* **2014**, *115*, 884–896.

Disclaimer/Publisher's Note: The statements, opinions and data contained in all publications are solely those of the individual author(s) and contributor(s) and not of MDPI and/or the editor(s). MDPI and/or the editor(s) disclaim responsibility for any injury to people or property resulting from any ideas, methods, instructions or products referred to in the content.